Inorganic Chemistry

ARTICLE

pubs.acs.org/IC

# Formation and Reactivity of a Porphyrin Iridium Hydride in Water: Acid Dissociation Constants and Equilibrium Thermodynamics Relevant to Ir−H, Ir−OH, and Ir−$CH_2$− Bond Dissociation Energetics

Salome Bhagan and Bradford B. Wayland*

Department of Chemistry, Temple University, 130 Beury Hall, 1901 North 13th Street, Philadelphia, Pennsylvania 19122, United States

Supporting Information

**ABSTRACT:** Aqueous solutions of group nine metal(III) (M = Co, Rh, Ir) complexes of tetra(3,5-disulfonatomesityl)porphyrin [(TMPS)$M^{III}$] form an equilibrium distribution of aquo and hydroxo complexes ($[(TMPS)M^{III}(D_2O)_{2-n}(OD)_n]^{(7+n)-}$). Evaluation of acid dissociation constants for coordinated water show that the extent of proton dissociation from water increases regularly on moving down the group from cobalt to iridium, which is consistent with the expected order of increasing metal−ligand bond strengths. Aqueous ($D_2O$) solutions of $[(TMPS)Ir^{III}(D_2O)_2]^{7-}$ react with dihydrogen to form an iridium hydride complex ($[(TMPS)Ir-D(D_2O)]^{8-}$) with an acid dissociation constant of $1.8(0.5) \times 10^{-12}$ (298 K), which is much smaller than the Rh−D derivative $(4.3\ (0.4) \times 10^{-8})$, reflecting a stronger Ir−D bond. The iridium hydride complex adds with ethene and acetaldehyde to form organometallic derivatives $[(TMPS)Ir-CH_2CH_2D(D_2O)]^{8-}$ and $[(TMPS)Ir-CH(OD)CH_3(D_2O)]^{8-}$. Only a six-coordinate carbonyl complex $[(TMPS)Ir-D(CO)]^{8-}$ is observed for reaction of the Ir−D with CO ($P_{CO}$ = 0.2−2.0 atm), which contrasts with the (TMPS)Rh−D analog which reacts with CO to produce an equilibrium with a rhodium formyl complex ($[(TMPS)Rh-CDO(D_2O)]^{8-}$). Reactivity studies and equilibrium thermodynamic measurements were used to discuss the relative M−X bond energetics (M = Rh, Ir; X = H, OH, and $CH_2$−) and the thermodynamically favorable oxidative addition of water with the (TMPS)Ir(II) derivatives.

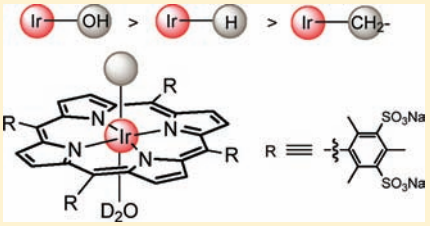


## INTRODUCTION

Water as a reaction medium and as a reactant for transition-metal-induced transformations and catalysis is a major contemporary topic[1−20] and a projected area for future growth.[21−23] Our contributions in this area have been focused on the behavior of group nine (Co, Rh, Ir) metal complexes with sulfonated porphyrin ligands in water[24−29] and methanol.[30−35] Primary objectives for these studies have encompassed defining the nature and thermodynamic interrelationships for species in solution, establishing the range of small molecule reactivity, and identifying prominent reaction pathways.

Rhodium porphyrins have a highly developed and extensive reaction chemistry in diverse reaction media[31,34,36−66] compared with studies of the iridium derivatives,[24,41,67−79] which are in a relatively early stage of development. Prior studies in this series have examined the equilibrium between group nine metalloporphyrin aquo and hydroxo complexes in water, reactions of rhodium(III) with hydrogen to form equilibrium distributions of Rh−H and Rh(I) species, and the reactivity patterns and thermodynamics for small molecule substrate reactions of Rh(I), Rh(II), Rh(III), and Rh−H derivatives.[27,28,80−83]

Oxidative addition of water to Rh(II)porphyrins, formation of $\beta$-hydroxyalkyl complexes from reactions of olefins with Rh(III), and reactions of the Rh−H with olefins, aldehydes, and CO that produce alkyl, $\alpha$-hydroxyalkyl, and formyl (Rh−CHO) complexes are important types of transformations observed in aqueous media. Free energy changes for most substrate reactions of rhodium porphyrins in water are remarkably similar to those for analogous reactions in hydrocarbon media with the exception of addition of Rh−H to alkenes where formation of highly hydrophobic alkyl groups is much less favorable in water.[28,84] Substrate reactions of (por)Rh−H are generally much faster in water compared to benzene which is ascribed to more versatile reaction pathways and in particular the capability of water to support ionic species and heterolysis routes.[28,84]

This article reports on reactivity and thermodynamic studies for aqueous solutions of tetra(3,5-disulfonatomesityl)porphyrin iridium(III) aquo and hydroxo complexes ($[(TMPS)M^{III}(D_2O)_{2-n}(OD)_n]^{(7+n)-}$) in $D_2O$. The (TMPS)Ir system was selected for study because the steric demands of the mesityl derivative inhibit Ir−Ir bonding and suppress intermolecular interactions that can occur for the less sterically demanding tetra(*p*-sulfonatophenyl)porphyrin (TSPP) derivative. The Ir(III) complex reacts with $H_2(D_2)$ to form a hydride complex ($[(TMPS)Ir^{III}-D(D_2O)]^{8-}$) that reacts with olefins and aldehydes to form iridium alkyl and $\alpha$-hydroxyalkyl complexes, but CO reacts to form only a carbon monoxide complex $[(TMPS)Ir-D(CO)]^{8-}$ without observation of an iridium formyl species (Ir−CHO). Results from equilibrium thermodynamic studies are used in discussing relative Ir−H, Ir−OH, and Ir−$CH_2$− bond dissociation energetics in water and free energy favorable (exergonic) oxidative addition of water with iridium(II) porphyrins.

**Received:** July 20, 2011
**Published:** October 14, 2011

## RESULTS AND DISCUSSION

**Aquo and Hydroxo Complexes of (TMPS)Ir$^{III}$ in Water.** Dissolution of the hydrated tetra(3,5-disulfonatomesityl)porphyrin iridium(III) complex ($Na_7[(TMPS)Ir^{III}(D_2O)_2]\cdot 18D_2O$) in $D_2O$ results in an equilibrium distribution of the bis-aquo complex ($[(TMPS)Ir^{III}(D_2O)_2]^{7-}$) (**1**) with mono- and bis-hydroxo complexes $[(TMPS)Ir^{III}(OD)(D_2O)]^{8-}$ (**2**) and $[(TMPS)Ir^{III}(OD)_2]^{9-}$ (**3**) (eqs 1 and 2) (Figure 1). The axially coordinated water and hydroxide ligands for **1**, **2**, and **3** in aqueous media rapidly interchange protons with the bulk water (298 K), which results in a single mole fraction averaged pyrrole $^1$H NMR resonance for **1**, **2**, and **3** (Figure 2).

$$[(TMPS)Ir^{III}(D_2O)_2]^{7-} \rightleftharpoons [(TMPS)Ir^{III}(OD)(D_2O)]^{8-} + D^+ \quad (1)$$

$$[(TMPS)Ir^{III}(OD)(D_2O)]^{8-} \rightleftharpoons [(TMPS)Ir^{III}(OD)_2]^{9-} + D^+ \quad (2)$$

$^1$H NMR spectra of the bis-aquo (**1**) and bis-hydroxo (**3**) complexes are directly observed at limiting low and high pD, respectively. The mole fraction averaged pyrrole $^1$H NMR resonances for equilibrium distributions of **1**, **2**, and **3** as a function of $[D^+]$ (Figure 2) were used in determining the acid dissociation constants for reactions 1 and 2 from nonlinear least-squares curve fitting giving the expression $\delta 2,3,4_{(obs)}(pyr) = (K_1K_2\delta_3(pyr) + K_1[D^+]\delta_2(pyr) + [D^+]^2\delta_1(pyr))/(K_1K_2 + K_1[D^+] + [D^+]^2)$ ($K_1$(298 K) = 2.8 × $10^{-8}$, $K_2$(298 K) = 2.5 × $10^{-11}$ and ($\delta_1$(pyr) = 8.63 ppm, $\delta_3$(pyr) = 8.27 ppm) (Table 2).[27,85] The equilibrium distribution of **1**, **2**, and **3** in $D_2O$ as a function of the hydrogen-ion concentration is illustrated in Figure 2b.

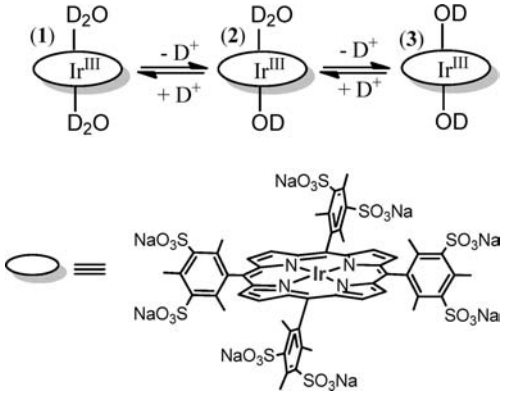


**Figure 1.** Water and hydroxide complexes of (TMPS) Ir$^{III}$ in water ($D_2O$).

**Comparison of Acid Dissociation Constants for Coordinated $D_2O$ in $[(TMPS)M(D_2O)_2]^{7-}$ Complexes in Water (M = Co, Rh, Ir).** Results from evaluation of the acid dissociation constants for coordinated water in aquo and hydroxo complexes of $[(TMPS)M^{III}]$ (M = Co, Rh, Ir) in $D_2O$ using $^1$H NMR are given in Table 1. The relative acidities of the $[(TMPS)M^{III}(D_2O)_2]^{7-}$ (M = Co, Rh, Ir) complexes increase regularly proceeding down group nine from Co to Ir, which reflects the expected trend of increasing metal−water ligand bond strengths.[86−88] Substitution of TMPS for TSPP results in a decrease in the corresponding acid dissociation constants for $[(TMPS)M^{III}(D_2O)_2]^{7-}$ (M = Co, Rh, Ir) (Table 1), which is consistent with the increased electron-releasing property of TMPS and decreased positive charge on the metal center relative to the TSPP complexes (Table 1). Sensitivity of the acid dissociation constants to changing the porphyrin from TMPS to TSPP decreases markedly going down group nine from cobalt to iridium (Table 1).

$$[(TMPS)M^{III}(D_2O)_2]^{7-} + OD^- \rightleftharpoons [(TMPS)M^{III}(OD)(D_2O)]^{8-} + D_2O \quad (3)$$

$$[(TMPS)M^{III}(OD)(D_2O)]^{8-} + OD^- \rightleftharpoons [(TMPS)M^{III}(OD)_2]^{9-} + D_2O \quad (4)$$

$$D_2O \rightleftharpoons D^+ + OD^- \quad (5)$$

The free energy changes for displacement of water by hydroxide for $[(TMPS)M^{III}(D_2O)_2]^{7-}$ (M = Co, Rh,[26] Ir) complexes are derived using reactions 1 and 2 along with the free energy for dissociation of $D_2O$ (eq 5) ($\Delta G_3^\circ = \Delta G_1^\circ - \Delta G_5^\circ$, $\Delta G_4^\circ = \Delta G_2^\circ - \Delta G_5^\circ$, where $\Delta G_5^\circ$ = 22.6 kcal mol$^{-1}$) . The binding of hydroxide is substantially more favorable than water in all cases, and the difference increases when moving down group nine from

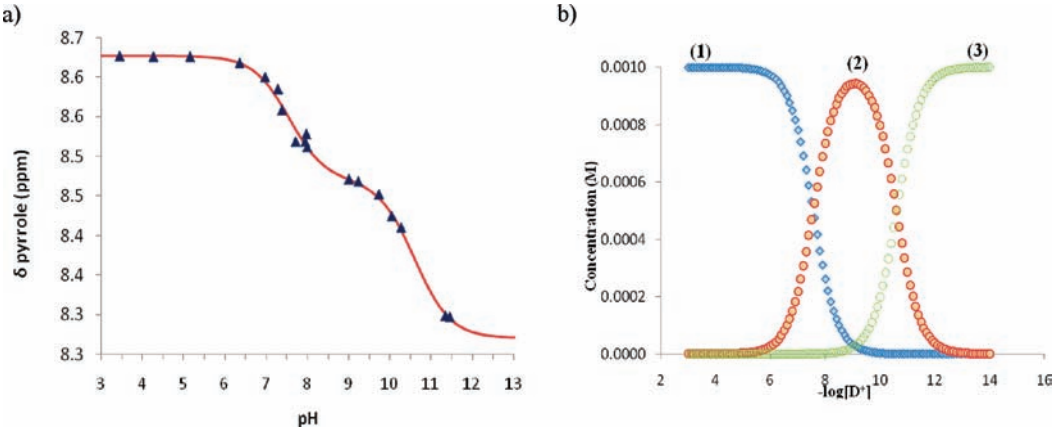


**Figure 2.** (a) Observed limiting fast exchange mole fraction averaged pyrrole $^1$H NMR chemical shifts for $[(TMPS)Ir^{III}(D_2O)_{2-n}(OD)_n]^{(7-n)-}$ complexes **1**, **2**, and **3** in $D_2O$. Points are experimentally determined values, and lines are calculated for $K_1$(298 K) = 2.8 × $10^{-8}$ and $K_2$(298 K) = 2.5 × $10^{-11}$. (b) Equilibrium distributions of **1**, **2**, and **3** as a function of the hydrogen-ion concentration in $D_2O$ at 298 K calculated for $K_1$(298 K) = 2.8 × $10^{-8}$ and $K_2$(298 K) = 2.5 × $10^{-11}$; total $[(TMPS)Ir^{III}]$ = 1.0 × $10^{-3}$ M.


dx.doi.org/10.1021/ic201553k |Inorg. Chem. 2011, 50, 11011–11020

**Table 1. First and Second Acid Dissociation Constants of Water ($K_1$, $K_2$) (298 K) and Free Energy Changes ($\Delta G_1°$, $\Delta G_2°$) (kcal/mol) (298 K) for $[(L)M^{III}(D_2O)]_2]^{7-}$ (L = TSPP, TMPS) (M = Co, Rh, Ir)[a] in $D_2O$**

| | TSPP | | | | TMPS | | | |
|---|---|---|---|---|---|---|---|---|
| $M^{III}$ | $K_1$ | $\Delta G_1°$ | $K_2$ | $\Delta G_2°$ | $K_1$ | $\Delta G_1°$ | $K_2$ | $\Delta G_2°$ |
| Co | $8.8 \times 10^{-9}$ | +10.9 | $7.1 \times 10^{-13}$ | +16.4 | $2.0 \times 10^{-10}$ | +13.2 | $2.5 \times 10^{-14}$ | +18.5 |
| Rh | $1.4 \times 10^{-8}$ | +10.6 | $2.8 \times 10^{-12}$ | +15.6 | $1.0 \times 10^{-9}$ | +12.3 | $2.8 \times 10^{-13}$ | +17.1 |
| Ir | $4.8 \times 10^{-8}$ | +9.90 | $2.6 \times 10^{-11}$ | +14.3 | $2.8 \times 10^{-8}$ | +10.3 | $2.5 \times 10^{-11}$ | +14.5 |

[a] References for previously reported values (TSPP)Rh,[27] (TSPP)Ir,[24] (TMPS)Rh.[25]

**Table 2. Free Energy Changes ($\Delta G_3°$, $\Delta G_4°$ (298 K) (kcal/mol)) for Reactions 3 and 4 That Substitute Hydroxide for Water in Complex $[(L)M^{III}(D_2O)]_2]^{7-}$ (L = TSPP, TMPS; M = Co, Rh, Ir) in $D_2O$**

| | TSPP | | TMPS | |
|---|---|---|---|---|
| $[(L)M^{III}(D_2O)_2]^{7-}$ | $\Delta G_3°$ | $\Delta G_4°$ | $\Delta G_3°$ | $\Delta G_4°$ |
| Co | −11.7 | −6.1 | −9.4 | −4.1 |
| Rh | −12.0 | −6.8 | −10.3 | −5.5 |
| Ir | −13.7 | −8.2 | −12.3 | −8.1 |

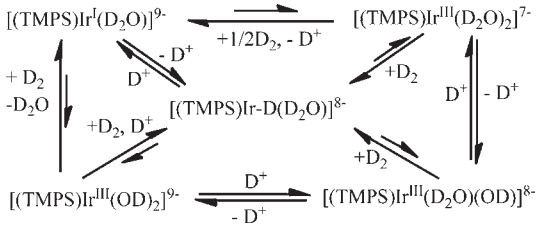


**Figure 3.** Simultaneous equilibria that occur between iridium porphyrin species from reaction of $[(TMPS)Ir(D_2O)_2]^{7-}$ with $D_2$ in $D_2O$ solution.

cobalt to iridium and is further increased for the less electron-donating porphyrin (TSPP), where there is a larger net positive charge on the metal center (Table 2).

**Reaction of (TMPS)Ir$^{III}$ Species with $H_2/D_2$ in $D_2O$.** Aqueous solutions of tetra(3,5-disulfonatomesityl)porphyrin iridium(III) react with hydrogen to produce equilibrium distributions between five iridium species including iridium hydride, iridium(I), and three iridium(III) aquo and hydroxo complexes that depend on the hydrogen-ion and dihydrogen concentrations (Figure 3).

**Equilibrium Constant To Form Ir−D from Reaction of [(TMPS)Ir$^{III}$(D$_2$O)$_2$]$^{7-}$ with $D_2/H_2$ in $D_2O$.** The bisaquo complex (**1**) reacts slowly with $H_2/D_2$ ($P(H_2) \approx 0.6-0.9$ atm) at relatively high hydrogen-ion concentrations ($[D^+] > 10^{-3}$) to produce an equilibrium distribution with the iridium hydride $[(TMPS)Ir-D(D_2O)]^{8-}$ (**5**) (eq 6)

$$[(TMPS)Ir^{III}(D_2O)_2]^{7-} + D_2 \rightleftharpoons [(TMPS)Ir-D(D_2O)]^{8-} + D^+ + D_2O \quad (6)$$

The equilibrium constant (298 K) for reaction 6 ($K_6 = 1.7$ (1.0), $\Delta G_6° = -0.3$ kcal/mol) was directly evaluated by integration of the $^1$H NMR for **1** and **5** in combination with the proton concentration $[D^+]$ and the solubility of $D_2$ in water[89] (Figure 4; Table 3). Dissolution of $[(TMPS)Ir-D(D_2O)]^{8-}$ (**5**) in $H_2O/D_2O$ (92:8) at pH 5−6 resulted in the observation of the very high field iridium hydride $^1$H NMR resonance at −59.1 ppm, which is permitted by the limiting slow exchange of Ir−D with $D_2O$. Exceptionally high-field $^1$H NMR positions for iridium hydrides compared to rhodium hydrides is one of the consequences of larger relativistic effects for iridium complexes.[90] Observation of the inequivalence of the *o*-Me groups by $^1$H NMR of **5** is also a manifestation of the slow proton exchange with water,[50] which is distinctly different from the fast proton exchange observed for $[(TMPS)Rh-D(D_2O)]^{8-}$ complex in water ($D_2O$).[25]

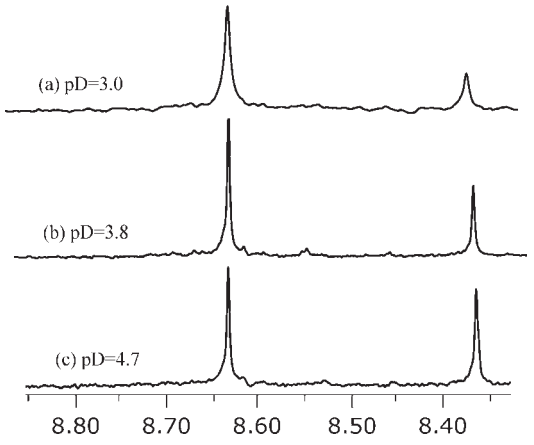


**Figure 4.** Hydrogen-ion dependence of the equilibrium of $[(TMPS)Ir^{III}(D_2O)_2]^{7-}$ shown at 8.63 ppm and $[(TMPS)Ir-D(D_2O)]^{8-}$ shown at 8.36 ppm.

Equilibrium thermodynamics for reactions of $[(TMPS)Ir^{III}(OD)(D_2O)]^{8-}$ (**2**) (eq 7) and $[(TMPS)Ir^{III}(OD)_2]^{9-}$ (**3**) (eq 8) with $H_2/D_2$ in water to form $[(TMPS)Ir-D(D_2O)]^{8-}$ (**5**) can be derived ($K_7 = K_6K_1^{-1}$; $K_8 = K_6K_1^{-1}K_2^{-1}$) (Table 3). Reaction of the iridium(III) complexes with hydrogen becomes more exergonic in basic aqueous media.

$$[(M^{III}(OD)(D_2O)]^{8-} + D_2 \rightleftharpoons [M-D(D_2O)]^{8-} + D_2O \quad (7)$$

$$[(M^{III}(OD)_2]^{9-} + D_2 + D^+ \rightleftharpoons [M-D(D_2O)]^{8-} + D_2O \quad (8)$$

Solutions of iridium(III) porphyrin in strongly basic $D_2O$ ($[D^+] \approx 10^{-11}$) react with $H_2/D_2$ ($P(H_2) \approx 0.5-0.6$ atm) to form the iridium(I) complex, $[(TMPS)Ir^I(D_2O)]^{9-}$ (**4**). Complex **4** is readily identified by a relatively high-field pyrrole $^1$H NMR resonance ($\delta_4 = 7.99$ ppm) compared to iridium(III) complexes (8.63−8.47 ppm), which is a characteristic that results from the presence of the electron-rich metal site in the iridium(I) complex. Nucleophilic substitution reactions for **4** with alkyl halides that result


dx.doi.org/10.1021/ic201553k |*Inorg. Chem.* 2011, 50, 11011–11020

**Table 3. Measured (eqs 6 and 9) and Derived (eq 7, 8, and 11−13) Equilibrium Constants ($K_n$) and $\Delta G°$ (298 K) (kcal/mol) for (TMPS)M Reactions in $D_2O$ (where M = Rh,[25] Ir)**

| | rxns of [(TMPS)M] | | M = Rh[a] | M = Ir |
|---|---|---|---|---|
| eq 6 | $[(M^{III}(D_2O)_2]^{7-} + D_2 \rightleftharpoons [M-D(D_2O)]^{8-} + D^+ + D_2O$ | | $K_6 = 18.2$ | $K_6 = 1.7(1)$ |
| | | | $\Delta G_6° = -1.7$ | $\Delta G_6° = -0.3(0.3)$ |
| eq 7 | $[(M^{III}(OD)(D_2O)]^{8-} + D_2 \rightleftharpoons [M-D(D_2O)]^{8-} + D_2O$ | (7) | $K_7 = 1.8 \times 10^{10}$ | $K_7 = 6.1 \times 10^7$ |
| | | | $\Delta G_7° = -14.0$ | $\Delta G_7° = -10.6$ |
| eq 8 | $[(M^{III}(OD)_2]^{9-} + D_2 + D^+ \rightleftharpoons [M-D(D_2O)]^{8-} + D_2O$ | (8) | $K_8 = 6.5 \times 10^{22}$ | $K_8 = 2.4 \times 10^{18}$ |
| | | | $\Delta G_8° = -31.1$ | $\Delta G_8° = -25.1$ |
| eq 9 | $[M-D(D_2O)]^{8-} \rightleftharpoons [(M^I(D_2O)]^{8-} + D^+$ | | $K_9 = 4.3 \times 10^{-8}$ | $K_9 = 1.8(0.5) \times 10^{-1}$ |
| | | | $\Delta G_9° = +10.0$ | $^2\Delta G_9° = +16.0(0.3)$ |
| eq 10 | $D^+ + D^- \rightleftharpoons D_2$ | (10) | $K_{10} = 5.2 \times 10^{37}$ | |
| | | | $\Delta G_{10}° = -53.2$ | |
| eq 11 | $[(M^{III}(D_2O)_2]^{7-} + D^- \rightleftharpoons [M-D(D_2O)]^{8-} + D_2O$ | (11) | $K_{11} = 9.5 \times 10^{38}$ | $K_{11} = 8.8 \times 10^{37}$ |
| | | | $\Delta G_{11}° = -53.1$ | $\Delta G_{11}° = -51.7$ |
| eq 12 | $[(M^{III}(D_2O)_2]^{7-} + [(M^I(D_2O)]^{9-} \rightleftharpoons [(M^{III}(OD)(D_2O)]^{8-} [M-D(D_2O)]^{8-}$ | (12) | $K_{12} = 2.3 \times 10^{-2}$ | $K_{12} = 2.3 \times 10^4$ |
| | | | $\Delta G_{12}° = +2.2$ | $\Delta G_{12}° = -6.0$ |
| eq 13 | $[(M^{III}(D_2O)_2]^{7-} + [(M^I(D_2O)]^{9-} + D_2 \rightleftharpoons 2[M-D(D_2O)]^{8-} + D_2O$ | (13) | $K_{13} = 4.2 \times 10^8$ | $K_{13} = 1.4 \times 10^{12}$ |
| | | | $\Delta G_{13}° = -11.7$ | $\Delta G_{13}° = -16.6$ |

[a] (TMPS)Rh thermodynamic values derived from ref 25.

in forming alkyl complexes ($[(TMPS)Ir-R(D_2O)]^{8-}$) is characteristic of the iridium(I) species. The alkyl complexes are readily identified in $D_2O$ solutions by characteristic high-field $^1H$ NMR resonances for the alkyl groups (Supporting Information).

**Evaluation of the Ir−D Acid Dissociation Constant for $[(TMPS)Ir-D(D_2O)]^{8-}$ in Water.** The pyrrole $^1H$ NMR resonances for $[(TMPS)Ir^I(D_2O)]^{9-}$ (**4**) ($\delta_4$ = 7.99 ppm) and $[(TMPS)Ir-D(D_2O)]^{8-}$ (**5**) ($\delta_5$ = 8.36 ppm) are observed as separate sharp peaks in $D_2O$ (Figure 5). The pyrrole resonance positions for **4** and **5** are invariant to pH change, but the peak intensities for the resonances of **4** and **5** change in accord with the heterolytic dissociation equilibrium given by eq 9.

$$[(TMPS)Ir-D(D_2O)]^{8-} \rightleftharpoons [(TMPS)Ir^I(D_2O)]^{9-} + D^+ \qquad (9)$$

In the pD range of 11−12, both species **4** and **5** are observed at equilibrium. The acid dissociation constant of $[(TMPS)Ir-D(D_2O)]^{8-}$ (**5**) in $D_2O$ was determined directly by integration of the $^1H$ NMR ($K_9$(298 K) = $1.8 \times 10^{-12}$, $\Delta G°_9$(298 K) = +16.0 kcal mol$^{-1}$). The acid dissociation constant for the Rh−D analog[25] of **5** is more than 4 orders of magnitude larger than the iridium hydride (Table 3). The free energy change (298 K) for heterolytic dissociation of $D^+$ from $[(TMPS)Ir-D(D_2O)]^{8-}$ is 6 kcal mol$^{-1}$ larger than that of $[(TMPS)Rh-D(D_2O)]^{8-}$, which primarily results from the larger iridium hydride bond energy.

Equilibrium constants and standard free energy changes for displacement of water from complex **1** by hydroxide (eq 3, $\Delta G_3° = \Delta G_1° + \Delta G_5° = -12.3$ kcal/mol) or by hydride (eq 11, $\Delta G_{11}° = \Delta G_6° + \Delta G_{10}° = -51.7$ kcal/mol) are derived from measured thermodynamic values (Table 3). The qualitative interrelationships between the five species in simultaneous equilibria shown in Figure 3 were quantitatively evaluated by measuring the equilibrium constants. Results from thermodynamic measurements for the (TMPS)Ir system are found in Table 3 along with comparative values for the (TMPS)Rh system. The free energy changes for this set of reactions for group nine (Co, Rh, Ir) metalloporphyrins are shown in Figure 6 where the group nine (M = Co, Rh, Ir) bisaquo metalloporphyrin complexes are set at zero to define the relative energy scale. The free energy change associated with converting any given metalloporphyrin species to another species of the same metal in water by reactions of $D_2$, $D^+$, and $D_2O$ is visually illustrated by Figure 6. Utilizing the free energy change diagram (Figure 6), conversion

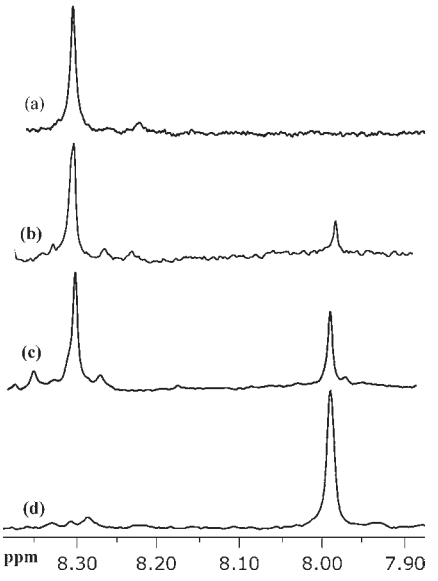


**Figure 5.** $^1H$ NMR (500 MHz) pyrrole resonances for aqueous solutions of $[(TMPS)Ir^I(D_2O)]^{9-}$ (**4**) and $[(TMPS)Ir-D(D_2O)]^{8-}$ (**5**) in $D_2O$ at pD = (a) 9.8, (b) 10.2, (c) 11.7, and (d) 12.5.


dx.doi.org/10.1021/ic201553k |*Inorg. Chem.* 2011, 50, 11011–11020

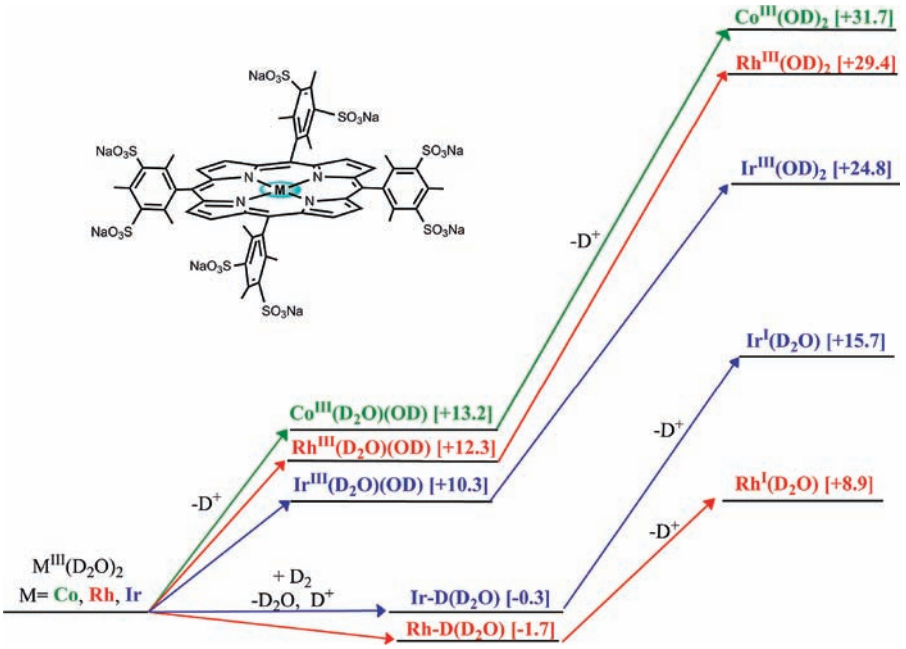


**Figure 6.** Free energy change ($\Delta G^{\circ}_{(298\ K)}$, kcal mol$^{-1}$) interrelationships diagram between $[(TMPS)M^{III}(D_2O)_2]^7$ (M = Co, Rh, Ir) complexes in $D_2O$.

of $[(TMPS)M^{III}(D_2O)(OD)]^{8-}$ to $[(TMPS)M^{I}(D_2O)]^{9-}$ is seen to be +3.4 and −5.4 kcal mol$^{-1}$, respectively, for rhodium and iridium and the increase in the energy of the systems by deprotonation is readily visualized.

**Evaluation of the Bond Dissociation Free Energy (BDFE) Difference between Ir−OD and Ir−D in $[(TMPS)Ir-X(D_2O)]^{8-}$ Complexes in $D_2O$.** The difference in the Ir−OD and Ir−D bond dissociation free energies (BDFE) can be evaluated from the standard free energy change for reaction 9, which is derived from experimental values for reaction 7 and the reverse of reaction 1 (Tables 1 and 3) ($K_9 = K_7/K_1 = 6.1 \times 10^7$, $\Delta G_9^{\circ} = -10.6$ kcal/mol; Tables 1 and 3). Using the BDFEs in $D_2O$ for D−D (103.4 kcal mol$^{-1}$) and D−OD (117.6 kcal mol$^{-1}$) the difference in the Ir−D and Ir−OD bond dissociation free energies is deduced by considering the bonds formed and broken in reaction 9 ($\Delta G_9^{\circ}$ = [Ir−OD] + [D−D] − [Ir−D] − [D−OD] and [Ir−OD]−[Ir−D] = $\Delta G_9^{\circ}$ + [D−OD] − [D−D]). The BDFE difference between (TMPS)Ir−OD and (TMPS)Ir−D is found to be 3.6 kcal mol$^{-1}$, which compares with a difference of only 0.2 kcal mol$^{-1}$ for (TMPS)Rh−OD and (TMPS)Rh−D.

$$[(TMPS)Ir^{III}(OD)(D_2O)]^{8-} + D_2 \rightleftharpoons [(TMPS)Ir-D(D_2O)]^{8-} + D_2O \quad (9)$$

We previously reported the BDFE difference between (TMPS)Rh−OD and (TMPS)Rh−D is 0.2 kcal mol$^{-1}$, and the corresponding difference for (TSPP)Rh−OD and (TSPP)Rh−D is 1.8 kcal mol$^{-1}$, Table 4. Evaluation of the difference in M−OD and M−D for (M = Rh, Ir) ([M−OD]−[M−D]) = $\Delta G_7^{\circ}$ + [(D−OD) − (D−D)] should be highly accurate because the equilibrium measurement of $\Delta G_9^{\circ}$ is within ±0.2 kcal mol$^{-1}$ and ([D−OD]−[D−D]) is constant (+14.2 kcal mol$^{-1}$). Table 5 provides values for the three systems where ([M−OD] − [M−D]) have been evaluated. In every example the [M−OD] BDFE in water is larger than the [M−D] BDFE but the difference varies from 3.6 to 0.2 kcal mol$^{-1}$ (Table 5). Variation in the $\pi$-acceptor interaction of the empty 6p orbitals orbital with the filled

**Table 4. Difference in BDFE (kcal mol$^{-1}$) between [(por)M−OD] and [(por)M−D)] (where por = TMPS, TSPP and M = Rh, Ir)**

| (por)M | (M−OD) − (M−D), kcal mol$^{-1}$ |
|---|---|
| (TMPS)Ir | 3.6 |
| (TMPS)Rh | 0.2 |
| (TSPP)Rh | 1.8 |

hydroxide oxygen $\pi$-donor orbitals is an interaction that could account for the changes in the difference in ([M−OD − [M−D]) BDFEs. A lower energy position for the 6p orbitals of iridium compared to rhodium and the corresponding stronger $\pi$ bonding with hydroxide could account for the increased spread of 3.4 kcal mol$^{-1}$ in ([M−OD] − [M−D]) BDFEs for the (TMPS)Ir complex compared to the (TMPS)Rh system, Table 5. Larger relativistic effects for iridium compared to rhodium result in a differential lowering of the 6s and 6p orbitals of Ir compared to Rh.[91,92] The larger spread of ([Rh−OD]−[Rh−D]) for the (TSPP)Rh compared to (TMPS)Rh system is consistent with a higher effective positive charge and lower energy 5p orbitals for the rhodium center in the (TSPP)Rh system.

**Implication for Oxidative Additions of Water with $(TMPS)Ir^{II}$.** Oxidative addition of water with transition-metal complexes is an important underinvestigated process that is a growing focus of attention.[21] The $\Delta G^{\circ}$ for oxidative addition of water ($D_2O$) with $[(TMPS)Rh^{II}(OD)(D_2O)]^{8-}$ is ca. −2.4 kcal mol$^{-1}$ (eq 14, M = Rh).[26]

$$2[(TMPS)M^{II}(D_2O)]^{8-} + D_2O \rightleftharpoons [(TMPS)M-D(D_2O)]^{8-} + [(TMPS)M-OD(D_2O)]^{9-} \quad (14)$$

The larger (TMPS)Ir−D compare to (TMPS)Rh−D of ∼4−6 kcal mol$^{-1}$ and an increase of (TMPS)Ir−OD relative to (TMPS)Rh−OD of 7−9 kcal mol$^{-1}$ makes oxidative addition of water highly


dx.doi.org/10.1021/ic201553k |Inorg. Chem. 2011, 50, 11011–11020

**Table 5. Measured and Derived Equilibrium Constants and Free Energy Changes for Reactions ($T$ = 298 K) of $[(TMPS)M-D(D_2O)]^{8-}$ (M = Rh,[25] Ir) with Unactivated Olefins and Acetaldehyde and CO**

| | (TMPS)M (M = Rh, Ir) | $K_n$ | $\Delta G°_n$ |
|---|---|---|---|
| eq 15 | $[Ir-D(D_2O)]^{8-} + C_2H_4 \rightleftharpoons [Ir-CH_2CH_2D(D_2O)]^{7-}$ | $5.1 \times 10^2$ | −3.7 |
| eq 16 | $[Ir-D(D_2O)]^{8-} + C_3H_6 \rightleftharpoons [Ir-CH_2CHDCH_3(D_2O)]^{7-}$ | $8.7 \times 10^1$ | −0.67 |
| | $[Rh-D(D_2O)]^{8-} + C_3H_6 \rightleftharpoons [Rh-CH_2CHDCH_3(D_2O)]^{7-}$ | $5.7 \times 10^3$ | −5.6 |
| eq 19 | $[Ir-D(D_2O)]^{8-} + HC(O)CH_3 \rightleftharpoons [Ir-CH(OD)CH_3(D_2O)]^{7-}$ | $9.5 \times 10^1$ | −2.7 |
| eq 20 | $[Ir-D(D_2O)]^{8-} + CO \rightleftharpoons [Ir-D(CO)]^{7-} + D_2O$ | $9.5 \times 10^3$ | −5.4 |
| | $[Rh-D(D_2O)]^{8-} + CO \rightleftharpoons [Rh-CDO(D_2O)]^{7-}$ | $1.7 \times 10^3$ | −4.4 |

favorable (M = Ir, $\Delta G°_{14} \approx -11$ to $-15$ kcal mol$^{-1}$) (eq 14). Although $[(TMPS)Ir^{II}(D_2O)]^{8-}$ and reaction 14 are not explicitly observed, properties of this process can be deduced from observation of reaction 12 and evaluation of thermodynamic values in Table 3 .

**Substrate Reactions of $[(TMPS)Ir-D(D_2O)]^{8-}$ with Olefins, Aldehydes, and Carbon Monoxide.** *Reaction of $[(TMPS)Ir-D(D_2O)]^{8-}$ with Olefins in Water.* Reaction of the iridium hydride (**5**) with terminal alkenes is very slow at acidic conditions but becomes faster as the pD increases ($[D^+] \approx 10^{-8}-10^{-11}$). Observation of higher reaction rates at basic conditions is ascribed to partial deprotonation of **5** to form equilibrium quantities of the reactive iridium(I) species $[(TMPS)Ir^{I}(D_2O)]^{9-}$. Aqueous solutions of the iridium hydride ($[(TMPS)Ir-D(D_2O)]^{8-}$) under basic conditions ($[D^+] > 10^{-10}$ M) react with ethene and propene to form measurable equilibrium concentrations of alkyl complexes in a period of 10 days (eqs 15 and 16)

$$[(TMPS)Ir-D(D_2O)]^{8-} + C_2H_4 \rightleftharpoons [(TMPS)Ir-CH_2CH_2D(D_2O)]^{8-} \quad (15)$$

$$[(TMPS)Ir-D(D_2O)]^{8-} + C_3H_6 \rightleftharpoons [(TMPS)Ir-CH_2CHDCH_3(D_2O)]^{8-} \quad (16)$$

The porphyrin ring current shifted high-field Ir−ethyl resonances of $[(TMPS)Ir-CH_2CH_2D(D_2O)]^{7-}$ (**6**) ($\delta$(Ir−$CH_2$CH$_2$D) = −5.68 ppm, $\delta$(Ir−CH$_2$$CH_2$D) = −1.85 ppm) and Ir−propyl peaks for $[(TMPS)Ir-CH_2CHDCH_3(D_2O)]^{7-}$ (**7**) ($\delta$(Ir−$CH_2$CHDCH$_3$) = −5.72 ppm, $\delta$(Ir−CH$_2$$CH$DCH$_3$) = −2.77 ppm, $\delta$(Ir−CH$_2$CHDC$H_3$) = −1.74 ppm) groups provide convenient observables to identify and quantify the Ir−alkyl species in $D_2O$. Addition of the iridium hydride to propene occurs with anti-Markovnikov regioselectivity, which places the iridium porphyrin on the less sterically demanding terminal primary carbon center.

Reactions of the alkenes with **5** (eqs 15 and 16) achieve a $^1$H NMR observable equilibrium which permitted evaluation of the equilibrium thermodynamics at 298 K ($K_{15} = 5.1 \times 10^2$, $\Delta G°_{15} = -3.7$ kcal mol$^{-1}$; $K_{16} = 8.7 \times 10^1$, $\Delta G°_{16} = -0.67$ kcal mol$^{-1}$; Table 5). The free energy changes for reactions of alkenes with the iridium hydride (Ir−D) (**5**) are 4−5 kcal mol$^{-1}$ less favorable than comparable porphyrin rhodium hydride (Rh−D) reactions in water (Table 5).[28] This is empirically associated with the increase in the iridium hydride BDFE (∼4−7 kcal mol$^{-1}$) compared to rhodium hydride that is not fully compensated by an increase in the Ir−$CH_2$− relative to the Rh−$CH_2$−.

*Catalytic Hydrogenation of Ethene.* A preformed sample of $[(TMPS)Ir-D(D_2O)]^{8}$ (**5**) ($5 \times 10^{-3}$ M) in acidic $D_2O$ (pD ≈ 3) when pressurized with ethene ($P(C_2H_4)$ = 600 Torr) and hydrogen ($P(H_2)$ = 500 Torr) results in the appearance of the ethyl organometallic **6** (eq 15) and ethane in the $^1$H NMR. Ethane is observed to be formed in a slow catalytic process in which 2.4 turnovers occur during the first hour at 298 K. Only qualitative conversion with time measurements could be achieved with this experimental design because of complications from producing a gaseous ethane product and the slow redistribution of reagents between the gas and the solution phases in the vacuum-adapted NMR tube. The process requires about 1 week to consume the hydrogen as the limiting reagent.

Catalytic hydrogenation of ethene probably occurs though the intermediacy of the ethyl complex ($[(TMPS)Ir-CH_2CH_2D-(D_2O)]^{8-}$), which reacts either in a concerted manner by a $\sigma$-bond metathesis type process with $H_2$ (eq 17) or by stepwise protonation and hydrogenation (eqs 18 and 6). The concerted pathway is currently preferred because independent study of reaction 6 at acid conditions indicates hydrogenation is far too slow to account for the observed ethane formation. A concerted $\sigma$-bond metathesis-type reaction for an iridium complex that does not have a readily available cis-coordination site has been previously illustrated by Milstein.[93]

$$[(TMPS)Ir-CH_2CH_2D(D_2O)]^{8-} + H_2 \rightleftharpoons C_2H_5D + [(TMPS)Ir-H(D_2O)]^{8-} + H^+ \quad (17)$$

$$[(TMPS)Ir-CH_2CH_2D(D_2O)]^{8-} + D^+ + D_2O \rightleftharpoons [(TMPS)Ir(D_2O)_2]^{7-} + C_2H_4D_2 \quad (18)$$

$$[(TMPS)Ir(D_2O)_2]^{7-} + H_2 \rightleftharpoons [(TMPS)Ir-H(D_2O)]^{8-} + H^+ + D_2O \quad (6)$$

*Reaction of $[(TMPS)Ir-D(D_2O)]^{8-}$ with Acetaldehyde.* Reaction of acetaldehyde with basic solutions ($[D^+] > 10^{-10}$ M) of $[(TMPS)Ir-D(D_2O)]^{8-}$ in $D_2O$ result in the $^1$H NMR observations of a doublet at −3.56 ppm and a broad resonance at −2.83 ppm indicative of formation of $[(TMPS)Ir-CH(OD)-CH_3(D_2O)]^{7-}$ (**9**) within 1 h. The organometallic is observed to be in equilibrium with **5** as shown in eq 19 ($K_{19}$= 9.5 × $10^1$, $\Delta G_{19}°$ = −2.7 kcal mol$^{-1}$).

$$[(TMPS)Ir-D(D_2O)]^{8-} + HC(O)CH_3 \rightleftharpoons [(TMPS)Ir-CH(OD)CH_3(D_2O)]^{7-} \quad (19)$$

*Reaction of $[(TMPS)Ir-D(D_2O)]^{8-}$ with CO.* The porphyrin pyrrole $^1$H NMR resonances for aqueous solutions of

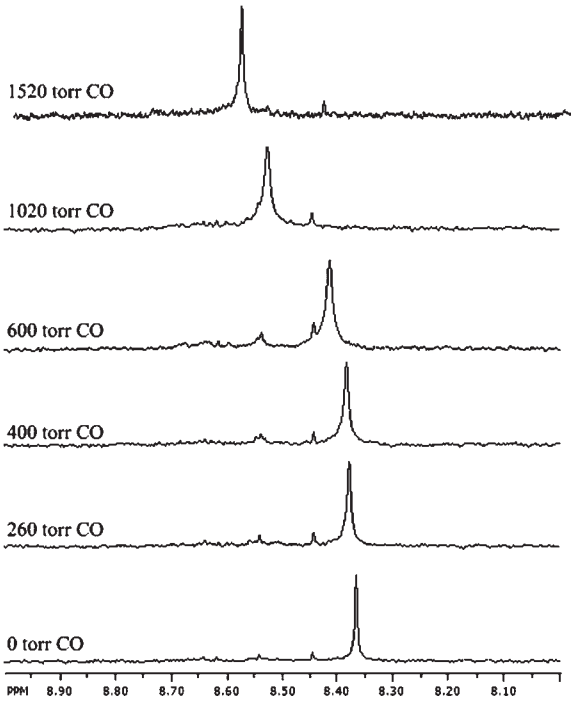


**Figure 7.** $^1$H NMR of mole fraction average pyrrole resonances of $[(TMPS)Ir{-}D(D_2O)]^{8-}$ and $[(TMPS)Ir{-}D(CO)]^{8-}$ in $D_2O$ at various CO pressures.

$[(TMPS)Ir{-}D(D_2O)]^{8-}$ in contact with CO are observed to shift regularly to lower field as the pressure of CO is increased. Changes in the porphyrin pyrrole resonances as a function of CO pressures are illustrated in Figure 7.

The pyrrole $^1$H NMR shifts are associated with mole fraction averaged positions that result from limiting fast exchange between $[(TMPS)Ir{-}D(D_2O)]^{8-}$ (**5**) and a CO complex ($[(TMPS)Ir{-}D(CO)]^{8-}$) (**10**), eq 20. The CO pressure dependence of the pyrrole $^1$H NMR position is accurately fitted to the equilibrium described by reaction 20 ($T$ = 298 K; $K_{20} = 9.5 \times 10^3$, $\Delta G°_{20}$= $-5.4$ kcal mol$^{-1}$) where the limiting pyrrole chemical shifts of **5** and **10** are 8.36 and 8.60 ppm, respectively.

$$[(TMPS)Ir{-}D(D_2O)]^{8-} + CO \rightleftharpoons [(TMPS)Ir{-}D(CO)]^{8-} + D_2O \quad (20)$$

In the same range of CO and metal porphyrin concentrations where $[(TMPS)Ir{-}D(D_2O)]^{8-}$ gives an equilibrium with a CO complex $[(TMPS)Ir{-}D(CO)]^{8-}$, the rhodium analog ($[(TMPS)Rh{-}D(D_2O)]^{8-}$) gives an equilibrium with a rhodium formyl complex $[(TMPS)Rh{-}CDO(D_2O)]^{8-}$, $K = 1.7 \times 10^3$, $\Delta G°$= $-4.4$ kcal mol$^{-1}$. Reaction of CO with the iridium hydride to produce a formyl complex (eq 21) must be thermodynamically less favorable than this process with the corresponding rhodium hydride.

$$[(TMPS)Ir{-}D(D_2O)]^{8-} + CO \rightleftharpoons [(TMPS)Ir{-}CDO(D_2O)]^{8-} \quad (21)$$

The BDFE for all Ir−X units is larger than the corresponding Rh−X BDFE, but the increase in the iridium hydride compared to the rhodium hydride is larger than the increase in Ir−C compared to Rh−C. Less favorable equilibrium thermodynamics for addition of the iridium hydride to ethene and propene compared to rhodium hydride by 4−5 kcal mol$^{-1}$ illustrates the larger increase in Ir−H compared to Ir−$CH_2$− relative to the rhodium derivative. The free energy change for reaction 21 to produce an iridium formyl falls short of that needed to give observable $^1$H NMR concentrations of $[(TMPS)Ir{-}CDO(D_2O)]^{8-}$, but modestly higher pressures of CO (∼50 atm) can be expected to give observable concentrations of the elusive iridium formyl complex.

## CONCLUSIONS

Aqueous solutions of group nine metal(III) (M = Co, Rh, Ir) complexes of tetra(3,5-disulfonatomesityl)porphyrin [(TMPS)M$^{III}$] form a hydrogen-ion-dependent equilibrium distribution of aquo and hydroxo complexes ($[(TMPS)M^{III}(D_2O)_{2-n}(OD)_n]^{(7+n)-}$). Evaluation of acid dissociation constants for coordinated water show that the extent of proton dissociation from coordinated water increases regularly on moving down the group from cobalt to iridium, which is consistent with increasing metal−water ligand binding. Aqueous ($D_2O$) solutions of $[(TMPS)Ir^{III}(D_2O)_2]^{7-}$ (**1**) react with dihydrogen to form an iridium hydride complex ($[(TMPS)Ir{-}D(D_2O)]^{8-}$) (**5**) with an acid dissociation constant of $1.8(0.5) \times 10^{-12}$ that is much smaller than the Rh−D derivative ($4.3\ (0.4) \times 10^{-8}$), reflecting a stronger Ir−D bond. The Ir−D unit in **5** adds with ethene and acetaldehyde to form organometallic derivatives $[Ir{-}CH_2CH_2D(D_2O)]^{7-}$ and $[Ir{-}CH(OD)CH_3(D_2O)]^{7-}$. Only a six-coordinate carbonyl complex $[(TMPS)Ir{-}D(CO)]^{8-}$ is observed for reaction of the hydride complex **5** with CO (0.2−2.0 atm), which contrasts with the (TMPS)Rh−D analog that forms a rhodium formyl complex at equilibrium. Reactivity studies and equilibrium thermodynamic measurements are used to deduce several features of the relative M−H, M−OH, and M−$CH_2$− BDFEs (M = Rh, Ir). (TMPS)Ir−D is approximately 4−6 kcal mol$^{-1}$ larger than (TMPS)Rh−D. The spread of the Ir−D, Ir−OD, and Ir−$CH_2$− BDFE values in water is substantially larger for the iridium system. The difference in the ($[(TMPS)Ir{-}OH] - [(TMPS)Ir{-}H]$) BDFEs and ($[(TMPS)Ir{-}CH_2{-}] - [(TMPS)Ir{-}D]$), respectively, differs by +3.4 and −4−5 kcal mol$^{-1}$ from the corresponding differences in BDFE values for the (TMPS)Rh system. Oxidative addition of water with (TMPS)Rh$^{II}$ has a $\Delta G°$ (298 K) of −2 kcal mol$^{-1}$, and the sum of the increases in the ((TMPS)Ir−OH) and ((TMPS)Ir−H BDFEs over those of the (TMPS)Rh system are approximately 12−16 kcal mol$^{-1}$, which permits deducing that the oxidative addition of water with (TMPS)Ir$^{II}$ is free energy favorable by ∼14−18 kcal mol$^{-1}$.

## EXPERIMENTAL SECTION

**General Considerations.** $D_2O$ was purchased from Cambridge Isotope Laboratory Inc. and degassed by three freeze−pump−thaw cycles before use. Proton NMR spectra were obtained on a Bruker Avance$^{III}$ 500 MHz at 293 K. Chemical shifts were referenced to 3-trimethyl silyl-1 propane sulfonic acid sodium salt. Proton NMR spectra were used to identify solution species and to determine the distribution of species at equilibrium. pH measurements are performed on Thermo Scientific XL15 m and Orion 9802 glass electrode[94] precalibrated by Thermo Orion buffer solutions of pH = 4.01, 7.00, and 10.01. Tetramesitylporphyrin (TMP) was synthesized according to the reported methods.[95−97] Sulfonation of *meso*-tetraphenylporphyrin sodium salt was achieved and subsequently purified by the method of Srivastava.[98] $Na_8[(TMPS)H_2]$ $^1$H NMR (500 MHz, $D_2O$) $\delta$(ppm): 8.58 (s, 8H, pyrrole), 3.23 (s, 12H, *p*-mesityl), 2.09 (s, 24H, *o*-mesityl), −2.35(s, br, 2H, −NH).

**Concentration of Complexes and Ionic Strength of Aqueous Solutions.** Thermodynamic studies of (TMPS)Ir complexes in water were carried out at concentrations less than $2 \times 10^{-3}$ M in order to minimize molecular and ionic association. Most equilibrium constant measurements were performed at a low ionic strength ($\mu \approx 10^{-3}$) where the ion activity coefficients approach unity.

**Synthesis of $Na_7[(TMPS)Ir^{III}(D_2O)_2]^{7-}$.** $Na_7[(TMPS)M^{III}(D_2O)_2]^{7-}$ (M = Co, Rh, Ir) was synthesized following the reported methods by Ashley.[13,14] $[Na_7(TMPS)Ir(D_2O)_2]$ was obtained by dissolving $Na_8(TMPS)H_2$ (100 mg, 0.06 mmol) and $[Ir(COD)Cl]_2$ (210 mg, 0.3 mmol) into 15 mL of methanol and refluxed for 5 days until complete metalation was determined by UV−vis. Two drops of 3% $H_2O_2$ water solution was used to oxidize iridium(I) to iridium(III). The solvent was removed under vacuum, and the product was purified on a silica column with methanol eluent to remove unreacted $[Ir(COD)Cl]_2$. Dissolution of **1** in $D_2O$ results in solutions of the bis aquo complex $[(TMPS)Ir^{III}(D_2O)_2]^{7-}$ (**1**) in an equilibrium distribution with the mono- and bis-hydroxo complexes, $[(TMPS)Ir^{III}(D_2O)(OD)]^{8-}$ (**2**) and $[(TMPS)Ir^{III}(OD)_2]^{9-}$ (**3**). $Na_7[(TMPS)Ir^{III}(D_2O)_2]$ $^1$H NMR (500 MHz, $D_2O$) $\delta$(ppm): 8.63 (s, 8H, pyrrole), 3.17 (s,12 H, *p*-methyl).2.17 (s, 24 H, *o*-methyl).

**Acid Dissociation Constant Measurement for $[(TMPS)M^{III}(D_2O)_2]^{7-}$ (M = Co, Ir) in Water.** Samples of ($[(TMPS)M^{III}(OD)_2]^{7-}$) (M = Co, Ir) were prepared by a mixing standardized $D_2O$ solution of NaOD with the stock solutions of complex **1** ($0.5-1.0 \times 10^{-3}$ M) in NMR tubes. A series of DCl and NaOD deuterium oxide solutions was used to tune the pH values. A plot of the pyrrole hydrogen $^1$H NMR chemical shifts to pD value (pD = pH + 0.41) and fit by nonlinear least-squares curve fitting to the equation

$$\delta_{2,3,4(obs)}(\text{pyr}) = \left(K_1K_2\delta_3(\text{pyr}) + K_1[D^+]2(\text{pyr}) + [D^+]^2\delta_1(\text{pyr})\right)/\left(K_1K_2 + K_1[D^+] + [D^+]^2\right)$$

**Synthesis of $[(TMPS)Ir-D(D_2O)]^{8-}$/$[(TMPS)Ir^{I}(D_2O)]^{9-}$.** A 0.4 mL amount of $[(TMPS)Ir^{III}(D_2O)_2]^{7-}$ $D_2O$ stock solutions ($1.2-1.8 \times 10^{-3}$ M, $[D^+] > 10^{-3}$ M) was added into a vacuum-adapted NMR tube. The NMR tubes were then degassed by three cycles of freeze−pump−thaw, and 500−700 Torr $H_2/D_2$ was pressurized into the NMR tube. Reaction of $[(TMPS)Ir^{III}(D_2O)_2]^{7-}$ with $H_2/D_2$ producing $[(TMPS)Ir-D]^{8-}$ in acidic solution achieves equilibrium distributions of $(TMPS)Ir^{III}$ and $[(TMPS)Ir-D]^{8-}$ species. The equilibrium constant was evaluated from the intensity integrations of $^1$H NMR of each species in combination with $D^+$ concentration measurement and the solubility of $H_2/D_2$ in water.[16] Following the same procedure, $(TMPS)Ir^{III}$ complexes completely converted to $[(TMPS)Ir^{I}]^{9-}$ in basic $D_2O$ solution ($[D^+] < 10^{-12}$ M). $[(TMPS)Ir-D(D_2O)]^{7-}$ $^1$H NMR (**5**) ($D_2O$, 500 MHz) $\delta$(ppm): 8.36 (s, 8H, pyrrole), 3.15 (s, 12H, *p*-methyl), 2.24 (s, 12 H, *o*-methyl), 2.15 (s, 12 H, *o*′-methyl). $[(TMPS)Ir^{I}(D_2O)]^{7-}$ $^1$H NMR (**4**) ($D_2O$, 500 MHz) $\delta$(ppm): 7.95 (s, 8H, pyrrole), 3.13 (s,12 H, *p*-methyl) 2.43 (s, 24 H, *o*-methyl).

**Acid Dissociation Constant Measurements for $[(TMPS)Ir-D(D_2O)]^{8-}$ in Water.** The acid dissociation constant of $[(TMPS)Ir-D(D_2O)]^{8-}$ was measured in water by direct observation of $[(TMPS)Ir-D(D_2O)]^{8-}$ and $[(TMPS)Ir^{I}(D_2O)]^{9-}$ concurrently between $[D^+]$ $10^{-10.5}$ and $10^{-12}$ in $^1$H NMR. Integration of the peak areas of **4** and **5** against a standard of known concentration was used to calculate the acid dissociation of eq 7 to give $K_7 = 1.8(0.5) \times 10^{-12}$, $\Delta G_7^\circ = +16.0(0.3)$ kcal/mol.

**Substrate Reactions of $[(TMPS)Ir-D(D_2O)]^{8-}$ and $[(TMPS)Ir^{I}(D_2O)]^{9-}$ with Olefins, Aldehydes, and CO in Water.** Substrate reactions of $[(TMPS)Ir-D]^{8-}$ and $[(TMPS)Ir^{I}]^{9-}$ with CO, aldehydes, and olefins in water were carried out by vacuum transfer of the substrate to vacuum line-adapted NMR tubes containing preformed samples of in $D_2O$ at a defined hydrogen-ion ($[D^+]$) concentration, and then dihydrogen was repressurized into the sample to suppress formation of $(TMPS)Ir^{III}$ species.

Proton NMR was used to identify solution species and to determine the distribution of each species at equilibrium. Equilibrium constants were evaluated from the intensity integrations of $^1$H NMR for each species in combination with $D^+$ concentration measurement and the solubility of the small organic substrate in water.[22] Equilibrium concentrations of $[(TMPS)Ir-D(D_2O)]^{8-}$ for the substrate reactions were determined from the averaged $^1$H NMR chemical shifts in combination with the $D^+$ ion concentration which determines the equilibrium distribution of $[(TMPS)Ir^{I}(D_2O)]^{9-}$ and $[(TMPS)Ir-D(D_2O)]^{8-}$.

**Reaction of $[(TMPS)Ir-D(D_2O)]^{8-}$ with CO.** A solution of $(TMPS)Ir^{III}$ ($10^{-3}$ M) was pressurized with a mixture of $H_2$/CO containing 70% of CO (0.6 atm) to form $[(TMPS)Ir-D(CO)]^{8-}$. The equilibrium constant is evaluated using least-squares averaging for the fast exchange mole fraction averaged iridium hyridic carbonyl and iridium hydride with limiting resonance $^1$H NMR shifts of 8.59 and 8.36 ppm, respectively. $[(TMPS)Ir-CO(D_2O)]^{8-}$ $^1$H NMR (500 MHz, $D_2O$) $\delta$(ppm): 8.59 (s, 8H, pyrrole), 3.16 (s, 12H, *p*-methyl), 2.17 (s, 12H, *o*-methyl), 2.13 (s, 12H, *o*′-methyl).

**Reaction of $[(TMPS)Ir-D(D_2O)]^{8-}$ with Ethene, Propene, and Acetaldehyde.** A solution of $[(TMPS)Ir-D(D_2O)]^{8-}$ ($3 \times 10^{-3}$ M) reacts with ethene and propene to form $[(TMPS)Ir-CH_2CH_2D(D_2O)]^{8-}$ and $[(TMPS)Ir-CH_2CHDCH_3(D_2O)]^{8-}$. Reactions of iridium hydride with all substrate olefins go to completion within the time needed to run a $^1$H NMR. Thermodynamic equilibrium constants are evaluated from integration of iridium alkyl complexes and iridium(I) in combination with the proton concentration which determines the equilibrium concentration of $[(TMSP)Ir-D(D_2O)]^{8-}$.

$^1$H NMR ($[(TMPS)Ir-CH_2CH_2D(D_2O)]^{8-}$) (500 MHz, $D_2O$) $\delta$(ppm): 8.29 (s, 8H, pyrrole), 3.20 (s, 12H, *p*-methyl), 2.16 (s, 24H, *o*-methyl), −1.85 (br, 2H,-$CH_2$), −5.68 (br, 2H, −$CH_2$D). ($[(TMPS)Ir-CH_2CHDCH_3(D_2O)]^{8-}$) $^1$H NMR (500 MHz, $D_2O$) $\delta$(ppm): 8.33 (s, 8H, pyrrole), 3.15 (s, 12H, *p*-methyl), 2.20(s, 24H, *o*-methyl), −5.72 (br, 2H, −$CH_2$CHDCH$_3$), −2.77 (br, 2H, −$CH_2$*CH*DCH$_3$), −1.74 (br, 2H, −$CH_2$CHDC$H_3$). ($[(TMPS)Ir-CH(OD)CH_3(D_2O)]^{8-}$) $^1$H NMR (500 MHz, $D_2O$; 292 K) $\delta$(ppm): 8.35 (s, 8H, pyrrole), 3.14 (s, 12H, *p*-methyl), 2.23 (s, 24H, *o*-methyl), −2.83 (br, 2H, −CH), −3.56(d, 3H, −$CH_3$, $J_{^1H-^1H}$ = 6.3 Hz).

**Reactions of $[(TMPS)Ir^{I}(D_2O)]^{9-}$ with RI (R= $CH_3$, $CH_2CH_3$, $(CH_2)_4CH_3$) in Water.** $[(TMPS)Ir-R(D_2O)]^{9-}$ (R = $CH_3$, $CH_2CH_3$, $(CH_2)_4CH_3$) was produced through transferring alkyl halide into the vacuum line-adapted NMR tube containing $[(TMPS)Ir^{I}(D_2O)]^{9-}$ solutions.

$[(TMPS)Ir-CH_3(OD)]^{9-}$ $^1$H NMR (500 MHz, $D_2O$) $\delta$(ppm): 8.26 (8H, pyrrole), 3.19 (s,12H, *p*-methyl), 2.38(s, 12H, *o*-methyl), 2.15(s, 12H, *o*′-methyl), −7.11 (br, 3H, $CH_3$).

$[(TMPS)Ir-CH_2CH_3(OD)]^{9-}$ $^1$H NMR (500 MHz, $D_2O$) $\delta$(ppm): 8.24 (8H, pyrrole), 3.19 (s,12H, *p*-methyl), 2.38(s, 12H, *o*-methyl), 2.15 (s, 12H, *o*′-methyl), −6.07 (br, 2H, $CH_2$), −3.96 (br, 3H, $CH_3$).

$[(TMPS)Ir-(CH_2)_4CH_3(OD)]^{9-}$ $^1$H NMR (500 MHz, $D_2O$) $\delta$(ppm): 8.23 (8H, pyrrole), 3.19 (s,12H, *p*-methyl), 2.40(s, 12H, *o*-methyl), 2.13(s, 12H, *o*′-methyl), −6.16 (t, 2H, C$H_2$−$(CH_2)_3CH_3$, $J_{^1H-^1H}$ = 7 Hz), −4.5 (t of d, 2H, $CH_2$−C$H_2$−$(CH_2)_2CH_3$, $J_{^1H-^1H}$ = 7 Hz, $J_{^1H-^1H}$ = 6.3 Hz), −1.33 (t, 2H, $(CH_2)_2$−C$H_2$−$CH_2CH_3$, $J_{^1H-^1H}$ = 6.3 Hz), −0.43 (br, 2H, $(CH_2)_3$-C$H_2CH_3$), −0.32 (br, 3H, $(CH_2)_4CH_3$).

## ■ ASSOCIATED CONTENT

**Supporting Information.** Calculations of equilibrium constants, tables and representative NMR spectra. This material is available free of charge via the Internet at http://pubs.acs.org.

## AUTHOR INFORMATION

**Corresponding Author**
*E-mail: bwayland@temple.edu.

## ACKNOWLEDGMENT

This research was supported by the Department of Energy, Division of Chemical Sciences and Office of Science through Grant DE-FG02-09ER-16000.

## REFERENCES

(1) Crabtree, R. H. *Organometallics* **2011**, *30*, 17.
(2) Piers, W. E. *Organometallics* **2011**, *30*, 13.
(3) Joo, F. *Acc. Chem. Res.* **2002**, *35*, 738.
(4) Campos-Malpartida, T.; Fekete, M.; Joo, F.; Katho, A.; Romerosa, A.; Saoud, M.; Wojtkow, W. *J. Organomet. Chem.* **2008**, *693*, 468.
(5) Almassy, A.; Nagy, C. E.; Benyei, A. C.; Joo, F. *Organometallics* **2010**, *29*, 2484.
(6) Taban-Caliskan, G.; Agustin, D.; Demirhan, F.; Vendier, L.; Poli, R. *Eur. J. Inorg. Chem.* **2009**, 5219.
(7) Dub, P. A.; Rodriguez-Zubiri, M.; Baudequin, C.; Poli, R. *Green Chem.* **2010**, *12*, 1392.
(8) Dinoi, C.; Ciclosi, M.; Manoury, E.; Maron, L.; Perrin, L.; Poli, R. *Chem.—Eur. J.* **2010**, *16*, 9572.
(9) Pryadun, R. S.; Atwood, J. D. *Organometallics* **2007**, *26*, 4830.
(10) Atwood, J. D. *J. Coord. Chem.* **2011**, *64*, 1.
(11) Burtscher, D.; Grela, K. *Angew. Chem., Int. Ed. Engl.* **2009**, *48*, 442.
(12) Labinger, J. A.; Bercaw, J. E. *Top. Organomet. Chem.* **2011**, *35*, 29.
(13) Chen, G. S.; Labinger, J. A.; Bercaw, J. E. *Organometallics* **2009**, *28*, 4899.
(14) Stahl, S. S.; Labinger, J. A.; Bercaw, J. E. *Ang. Chem. Int. Ed.* **1998**, *37*, 2181.
(15) McLaughlin, M. P.; McCormick, T. M.; Eisenberg, R.; Holland, P. L. *Chem. Commun.* **2011**, *47*, 7989.
(16) Jarosz, P.; Du, P.; Schneider, J.; Lee, S.-H.; McCamant, D.; Eisenberg, R. *Inorg. Chem.* **2009**, *48*, 9653.
(17) Postigo, A. *Curr. Org. Chem.* **2009**, *13*, 1683.
(18) Kim, S. B.; Cai, C.; Faust, M. D.; Trenkle, W. C.; Sweigart, D. A. *Organometallics* **2009**, *28*, 2625.
(19) Li, H.; Yin, H.; Zhang, F.; Li, H.; Huo, Y.; Lu, Y. *Environ. Sci. Technol.* **2009**, *43*, 188.
(20) Genet, J.-P.; Darses, S.; Michelet, V. *Pure Appl. Chem.* **2008**, *80*, 831.
(21) Ozerov, O. V. *Chem. Soc. Rev.* **2009**, *38*, 83.
(22) Eisenberg, R. *Science* **2009**, *324*, 44.
(23) Dempsey, J. L.; Esswein, A. J.; Manke, D. R.; Rosenthal, J.; Soper, J. D.; Nocera, D. G. *Inorg. Chem.* **2005**, *44*, 6879.
(24) Bhagan, S.; Sarkar, S.; Wayland, B. B. *Inorg. Chem.* **2010**, *49*, 6734.
(25) Fu, X.; Li, S.; Wayland, B. B. *J. Am. Chem. Soc.* **2006**, *128*, 8947.
(26) Fu, X.; Li, S.; Wayland, B. B. *Inorg. Chem.* **2006**, *45*, 9884.
(27) Fu, X.; Wayland, B. B. *J. Am. Chem. Soc.* **2004**, *126*, 2623.
(28) Fu, X.; Wayland, B. B. *J. Am. Chem. Soc.* **2005**, *127*, 16460.
(29) Li, Y.; Wayland, B. B. *Chem. Commun.* **2003**, 1594.
(30) Bosch, H. W.; Wayland, B. B. *Chem. Commun.* **1986**, 900.
(31) Cui, W.; Zhang, X. P.; Wayland, B. B. *J. Am. Chem. Soc.* **2003**, *125*, 4994.
(32) Cui, W. H.; Zhang, X. P.; Wayland, B. B. *J. Am. Chem. Soc.* **2003**, *125*, 4994.
(33) Li, S.; Sarkar, S.; Wayland, B. B. *Inorg. Chem.* **2009**, *48*, 8550.
(34) Sarkar, S.; Li, S.; Wayland, B. B. *J. Am. Chem. Soc.* **2010**, *132*, 13569.
(35) Sarkar, S.; Li, S.; Wayland, B. B. *Inorg. Chem.* **2011**, *50*, 3313.
(36) Bunn, A. G.; Wayland, B. B. *J. Am. Chem. Soc.* **1992**, *114*, 6917.
(37) Coffin, V. L.; Brennen, W.; Wayland, B. B. *J. Am. Chem. Soc.* **1988**, *110*, 6063.
(38) Cui, W.; Wayland, B. B. *J. Am. Chem. Soc.* **2004**, *126*, 8266.
(39) Cui, W.; Wayland, B. B. *J. Am. Chem. Soc.* **2006**, *128*, 10350.
(40) Del Rossi, K. J.; Wayland, B. B. *J. Am. Chem. Soc.* **1985**, *107*, 7941.
(41) Farnos, M. D.; Woods, B. A.; Wayland, B. B. *J. Am. Chem. Soc.* **1986**, *108*, 3659.
(42) Sherry, A. E.; Wayland, B. B. *J. Am. Chem. Soc.* **1989**, *111*, 5010.
(43) Sherry, A. E.; Wayland, B. B. *J. Am. Chem. Soc.* **1990**, *112*, 1259.
(44) Wayland, B. B.; Ba, S.; Sherry, A. E. *J. Am. Chem. Soc.* **1991**, *113*, 5305.
(45) Wayland, B. B.; Newman, A. R. *J. Am. Chem. Soc.* **1979**, *101*, 6472.
(46) Wayland, B. B.; Sherry, A. E.; Bunn, A. G. *J. Am. Chem. Soc.* **1993**, *115*, 7675.
(47) Wayland, B. B.; Sherry, A. E.; Poszmik, G.; Bunn, A. G. *J. Am. Chem. Soc.* **1992**, *114*, 1673.
(48) Wayland, B. B.; Van Voorhees, S. L.; Del Rossi, K. J. *J. Am. Chem. Soc.* **1987**, *109*, 6513.
(49) Wayland, B. B.; Woods, B. A.; Pierce, R. *J. Am. Chem. Soc.* **1982**, *104*, 302.
(50) Zhang, X.-X.; Parks, G. F.; Wayland, B. B. *J. Am. Chem. Soc.* **1997**, *119*, 7938.
(51) Zhang, X.-X.; Wayland, B. B. *J. Am. Chem. Soc.* **1994**, *116*, 7897.
(52) Choi, K. S.; Lai, T. H.; Lee, S. Y.; Chan, K. S. *Organometallics* **2011**, *30*, 2633.
(53) Fung, H. S.; Li, B. Z.; Chan, K. S. *Organometallics* **2010**, *29*, 4421.
(54) Choi, K. S.; Chiu, P. F.; Chan, K. S. *Organometallics* **2010**, *29*, 624.
(55) Au, C. C.; Lai, T. H.; Chan, K. S. *J. Organomet. Chem.* **2010**, *695*, 1370.
(56) Lai, T. H.; Chan, K. S. *Organometallics* **2009**, *28*, 6845.
(57) Fung, H. S.; Chan, Y. W.; Cheung, C. W.; Choi, K. S.; Lee, S. Y.; Qian, Y. Y.; Chan, K. S. *Organometallics* **2009**, *28*, 3981.
(58) Chan, Y. W.; Chan, K. S. *Organometallics* **2008**, *27*, 4625.
(59) Chan, K. S.; Mak, K. W.; Tse, M. K.; Yeung, S. K.; Li, B. Z.; Chan, Y. W. *J. Organomet. Chem.* **2008**, *693*, 399.
(60) Zhang, L.; Chan, K. S. *Organometallics* **2007**, *26*, 679.
(61) Zhang, L.; Chan, K. S. *J. Organomet. Chem.* **2007**, *692*, 2021.
(62) Biffinger, J. C.; Uppaluri, S.; Sun, H.; DiMagno, S. G. *ACS Catal.* **2011**, *1*, 764.
(63) Sun, H.; Xue, F.; Nelson Andrew, P.; Redepenning, J.; DiMagno Stephen, G. *Inorg. Chem.* **2003**, *42*, 4507.
(64) Nelson, A. P.; DiMagno, S. G. *J. Am. Chem. Soc.* **2000**, *122*, 8569.
(65) Wayland, B. B.; Ba, S.; Sherry, A. E. *Inorg. Chem.* **1992**, *31*, 148.
(66) Wayland, B. B.; Coffin, V. L.; Farnos, M. D. *Inorg. Chem.* **1988**, *27*, 2745.
(67) Li, B. Z.; Fung, H. S.; Song, X.; Chan, K. S. *Organometallics* **2011**, *30*, 1984.
(68) Cheung, C. W.; Chan, K. S. *Organometallics* **2011**, *30*, 1768.
(69) Li, B. Z.; Song, X.; Fung, H. S.; Chan, K. S. *Organometallics* **2010**, *29*, 2001.
(70) Lee, S. Y.; Cheung, C. W.; Hsu, I. J.; Chan, K. S. *Inorg. Chem.* **2010**, *49*, 9636.
(71) Cheung, C. W.; Fung, H. S.; Lee, S. Y.; Qian, Y. Y.; Chan, Y. W.; Chan, K. S. *Organometallics* **2010**, *29*, 1343.
(72) Li, B.; Chan, K. S. *Organometallics* **2008**, *27*, 4034.
(73) Cheung, C. W.; Chan, K. S. *Organometallics* **2008**, *27*, 3043.
(74) Cui, W.; Li, S.; Wayland, B. B. *J. Organomet. Chem.* **2007**, *692*, 3198.
(75) Del Rossi, K. J.; Zhang, X.-X.; Wayland, B. B. *J. Organomet. Chem.* **1995**, *504*, 47.
(76) Del Rossi, K. J.; Wayland, B. B. *Chem. Commun.* **1986**, 1653.
(77) Collman, J. P.; Kim, K. *J. Am. Chem. Soc.* **1986**, *108*, 7847.
(78) Collman, J. P.; Chng, L. L.; Tyvoll, D. A. *Inorg. Chem.* **1995**, *34*, 1311.
(79) Zhai, H.; Bunn, A.; Wayland, B. *Chem. Commun.* **2001**, 1294.
(80) Zhang, J.; Wayland, B. B.; Yun, L.; Li, S.; Fu, X. *Dalton Trans.* **2010**, *39*, 477.
(81) Li, S.; Sarkar, S.; Wayland, B. B. *Inorg. Chem.* **2009**, *48*, 8550.

(82) Fu, X.; Li, S.; Wayland, B. B. *J. Am. Chem. Soc.* **2006**, *128*, 8947.
(83) Fu, X.; Basickes, L.; Wayland, B. B. *Chem. Commun.* **2003**, 520.
(84) Fu, X.; Basickes, L.; Wayland, B. B. *Chem. Commun.* **2003**, 520.
(85) Sutter, T. P. G.; Rahimi, R.; Hambright, P.; Bommer, J. C.; Kumar, M.; Neta, P. *J. Chem. Soc., Faraday Trans* **1993**, *89*, 495.
(86) Hancock, R. D.; Martell, A. E. *Chem. Rev.* **1989**, *89*, 1875.
(87) Grossman, J. C.; Mizel, A.; Côté, M.; Cohen, M. L.; Louie, S. G. *Phys. Rev. B* **1999**, *60*, 6343.
(88) Tsuda, M.; Dy, E. S.; Kasai, H. *J. Chem. Phys.* **2005**, *122*, 2447191.
(89) In *Solubility of Gases in Liquids: A Critical Evaluation of Gas/Liquid Systems in Theory and Practice*; Fogg, P. G.T. G., W.,, Ed.; Wiley, 1991.
(90) Hrobárik, P.; Hrobáriková, V.; Meier, F.; Repiský, M.; Komorovský, S.; Kaupp, M. *J. Phys. Chem. A* **2011**, *115*, 5654.
(91) Elsasser, C.; T., N.; Ho, K. M,; Chan, C. T.; Braun, P.; Fahnle, M. *Phys.: Condens. Matter* **1990**, *2*, 4371.
(92) Pyykko, P. *Chem. Rev.* **1988**, *88*, 563.
(93) Blum, O.; Milstein, D. *J. Organomet. Chem.* **2000**, *593*−*594*, 479.
(94) Glasoe, P. K.; Long, F. A. *J. Phys. Chem.* **1960**, *64*, 188.
(95) Ashley, K. R.; Leipoldt, J. G. *Inorg. Chem.* **1981**, *20*, 2326.
(96) Ashley, K. R.; Shyu, S.-B.; Leipoldt, J. G. *Inorg. Chem.* **1980**, *19*, 1613.
(97) Lindsey, J. S.; Wagner, R. W. *J. Org. Chem.* **1989**, *54*, 828.
(98) Srivastava, T. S.; Tsutsui, M. *J. Org. Chem.* **1973**, *38*, 2103.